A New Perspective and Explanation for the Formation of Plasmaspheric Shoulder Structures

Hua Zhang [1]   Guangshai Peng[1]   Chao Shen [2]   Wu Yewen[1]

[1]Institute of Space Weather, Nanjing University of Information Science & Technology, Nanjing, China.

[2]Harbin Institute of Technology, Shen Zhen, China.

Correspondence to: Hua Zhang (289534957@qq.com)

Abstract

Over the hours of 5-9 UT on 8 June 2001, the extreme ultraviolet (EUV) instrument onboard IMAGE satellite observed a shoulder-like formation in the morning sector and a post-noon plume-like structure. The plasmapause formation is simulated using the Test Particle Model (TPM), based on a drift motion theory, which reproduces various plasmapause structures and evolution of the shoulder feature. The analysis indicates that the Shoulder is created by sharp reduction and spatial non-uniform in the dawn-dusk convection electric field intensity. The TPM modeled event is found to develop an initial pre-dawn asymmetric bulge that becomes a shoulder as a result of increased "co-rotation" rate with increasing L-shell that is preceded by localized outward convection. The shoulder structure rotates sunward and develops into a single or double plume structure during an active time period in simulation.

Keywords: plasmapause; shoulder-like; plume-like;IMAGE/EUV

1. Introduction

The plasmasphere is an important region in the inner magnetosphere, surrounding the Earth and extending to 5 Earth radii(Re), which contains dense(10-10000 cm^{-3}) and cold plasma (below 1ev). The plasmapause is formed by a superposition of corotation and convection electric field in the inner magnetosphere (Nishida, 1966; Chen and Wolf, 1972). The formation and size of plasmapause vary with a geomagnetic activity level. Generally, as the disturbance level increases, the plasmapause position moves closer to the Earth and of shape deviates from circle in

the equatorial plane (Grebowsky, 1970). Atypical plasmapause structures, such as 'bulge' and plume, occur often in both whistler and in-situ data (Carpenter and Anderson, 1992). There are many theoretical research studies to explain the formation of plume (Grebowsky, 1970; Pierrard and Lemaire, 2004; Zhang et al., 2013), and Pierrard and Cabrera (2006) firstly simulated a double-plume , but did not explain the origin of second-plume.

The EUV instrument onboard IMAGE satellite was launched in March 2000, that provided a global perspective of the plasmasphere. Such as plume, finger, notch and shoulder, and so on, were observed by EUV (Sandel et al., 2001). One of plasmaspheric structures, shoulder, has been less studied in the previous papers than plume. However, the shoulder may play an important role in a loss mechanism for ring current (Burch et al., 2001). So, it is important to study the formation mechanism of the shoulder.

At present, there are no convincing explanations for the dynamic formation of shoulder. Goldstein et al.(2002) firstly proposed an explanation, based on the Magnetospheric Specification Model(MCM) simulation output, for the formation of shoulder. They proposed that the shoulder is created by a sudden decrease of dusk-dawn electric field. As the interplanetary magnetic field (IMF) turns northward from southward, it triggers anti-sunward flow of plasma in the predawn sector, to produce an asymmetric bulge called shoulder. Later, based on physical mechanism of interchange instability and a Kp-dependent E5D electric field model, Pierrard and Lemaire (2004) suggested that the shoulder is not the result of radial outflow of plasma, same as the presentation of Goldstein et al. (2002), but is inward plasma drift in post-midnight sector.

Then, scarce papers about dynamical formation of the shoulder are delivered than of the plume. In this paper, we used TPM to simulate dynamical formation of the shoulder, using Weimer's statistical E-field (Weimer, 2001; Zhang et al., 2012), which is both spatially nonuniform and dynamically responsive to change geomagnetic and solar wind conditions. To drive the TPM model, several inputs are used: Dst, solar wind (SW) and interplanetary magnetic field (IMF) data sets. The

59   authors make an attempt to propose a new convincing explanation for the formation

60   of the shoulder-like structure, different from the previous explanations.

61   2. Shoulder Observation

62
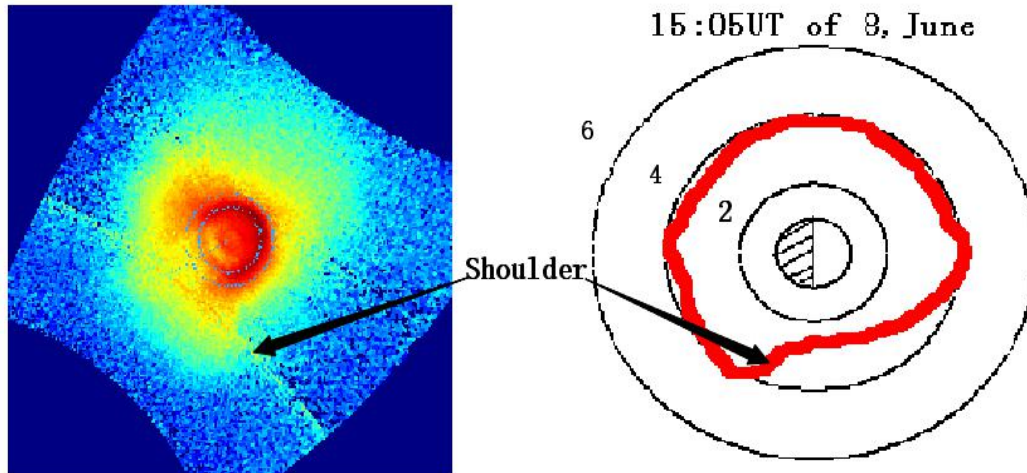
Figure1. Snapshot of plasmasphere (left panel) by EUV instrument, at 15:05 UT of 8 June 2001,

Sunlight is an incident from the upper right. Earth is in the center of panels and shoulder is

observed and labeled in the snapshot. The right panel is plasmapause that is extracted from the

left plasmapheric image.

67   Figure 1 illustrates the shoulder-like structure, a sharp radial plasmaspheric

68   structure about 1 RE radial extension, in the post-midnight sector, which was viewed

69   by EUV imager onboard IMAGE satellite at 15:05 UT of 8 June 2001. The right panel

70   illustrates the plasmapause extracted from the left panel in Figure 1. The outer

71   boundary of plasmasphere is assumed to be 40% of maximum brightness of 30.4nm

72   He^+ emission, where the intensity is the logarithm of the luminosity (Pierrard and

73   Cabrera, 2006). Then, the shoulder-like is labeled and marked by arrows in the plot.

74   Comparison of sequential observations with the simulation pictures, show that the

75   shoulder structure corotating with the main plasmaspheric body can be seen in Figure

76   3, and is discussed in the next section. That means the outer edge of the shoulder

77   corotates faster than the inner edge in development phase (Goldstein et al., 2002).

78   Then, the shoulder moves eastward to the afternoon sector and evolves into the

79   plume-like structure. Over the next hours, the outer body of plume flows sunward

80   from noon sector, and results in the plume thinning out and disappearing (can see the

81   simulation of Figure 3). In the next section, we take the case of 8 June 2001

82   observation as an example, to discuss the simulation of the Shoulder and the plume

83   evolution based on the TPM method.

3. Simulation

85   In the region of plasmasphere occupied, charged particles are cold plasma (e.g.

86   energy of particles is < 1eV). So, we can assume that plasma elements have only $\boldsymbol{E} \times$

87    $\boldsymbol{B}/B^2$ drift motions (Li and Xu, 2005; Lejosne and Mozer, 2016). Here, the electric

88   field intensity of E-model is superposition of convection and corotation electric field.

89   The electric field plays a key role in plasma drift motion and the formation of

90   plasmasphere (Pierrard et al., 2008). In the present paper, the Weimer's electric field

91   (Weimer, 2001) is mapped into the magnetosphere along magnetic lines to model the

92   magnetospheric convection electric field (Zhang et al., 2012), and T96 magnetic field

93   to model the background magnetic field.

94   In the simulation, the calculation region is radial range of 2-7 Re and azimuthal

95   span 0-359°. Dispersion by iso-spacing grids that correspond to the radial and

96   azimuthal steps are equal to 0.1Re and 1° respectively, in the magnetic equatorial

97   plane. Ten particles are placed into each grid, so particle density is proportional to L^{-1}

98   which is not consistent with the actual density in a saturation state (close to true

99   density presumably is proportional to L^{-4}), but is adequate to study the evolution of

100   plasmaspheric morphology using a skeleton map of particles during a substorm period.

101   The TMP runs 3 days under the low activity condition to obtain the boundary

102   conditions for the simulation.

103
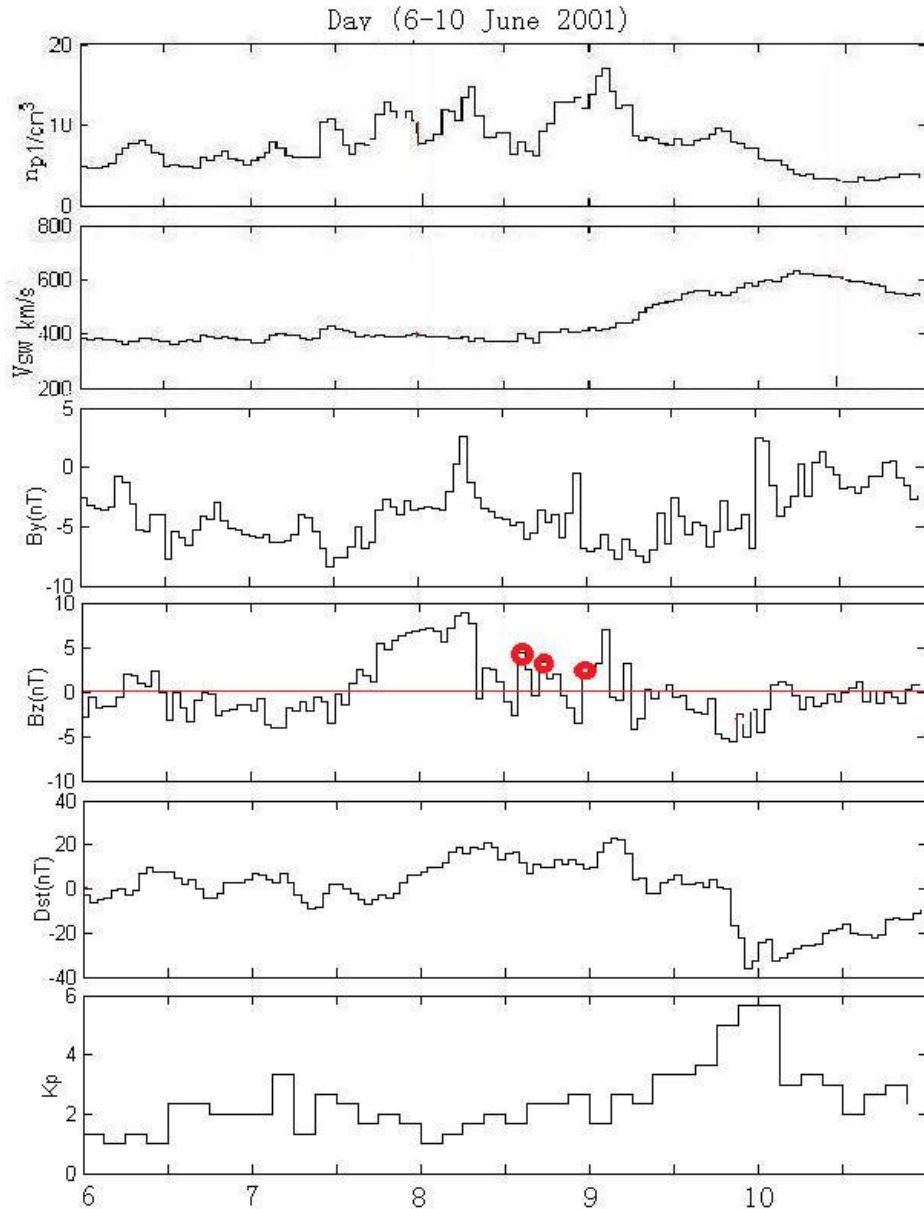
Figure 2. Input parameters of the TPM model, the variation of the By and Bz component of the

IMF, the Dst index and Kp index, on 6 -10 June 2001, is a typical substorm case.

The paper presents the case of 8-9 June 2001, to study the evolution of the shoulder and propose a hypothetical explanation produced by TPM simulation. During the geomagnetic substorm, all the TPM inputs are available. IMF and Solar Wind data are available in ACE satellite data center, and Dst index can be seen in World Data center for Geomagnetism, Kyoto. Fig.2 shows the By, Bz components of the IMF, the Dst index and the geomagnetic activity index Kp, observed from 6 to 10 June 2001. This is a typical substorm case where the Kp index gradually increases up to 5+ and then decreases. The TPM runs with

114   3-minute time resolution from 6 June at 00:00 UT to 10 June at 12:00 UT. The

115   results of simulation are shown in Fig.3, whose corresponding times are labeled

116   on the title of each panel. The simulated plasmapause is a skeleton which consists

117   of continuous particle distribution. Comparison of TPM simulation (black body)

118   and EUV observation (red line) in Fig.3 indicates that the simulated plasmapause

119   positions correspond generally rather favorable with the EUV observations. The

120   results of EUV observation show that the plasmapause is seldom smooth or

121   irregular, due to the fluctuations in plasmapause region caused by successive

122   particles injection during a disturbance period (Goldstein et al., 2002; Gallagher et

123   al., 2005), in agreement with previous whistler observations (Carpenter and

124   Anderson, 1992). In contrast, the simulation of plasmapauses by TPM is more

125   smooth. So, observations and simulations are not identical, due to deviation in the

126   extraction of the boundary from EUV image and optical contamination of the

127   image (Sandel et al., 2001; Zhang et al., 2013) and the limitation in the TPM

128   model and the unrealistic Weimer electric field model. .

129
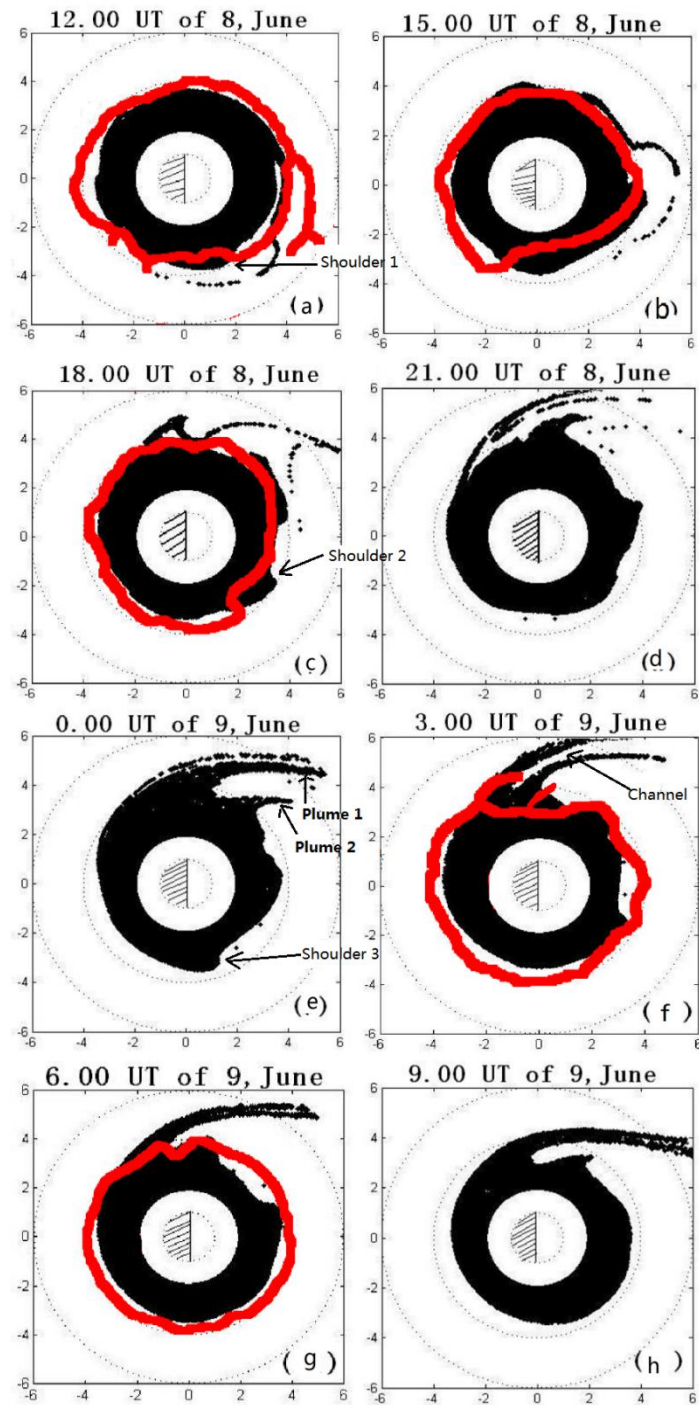
Figure 3. The simulation of plasmaspheric morphology compared with EUV/IMAGE observation in the geomagnetic equatorial plane on 8 - 9 June 2001. The red irregular curves indicate plasmapause observation by EUV/IMAGE. Black contours are the plasmasphere simulated by the TPM model. White contours are the main plasmasphere (located at 1-2 Re region). The dotted circles on the panels correspond to L=1, 2, 4 and 6.

135

136
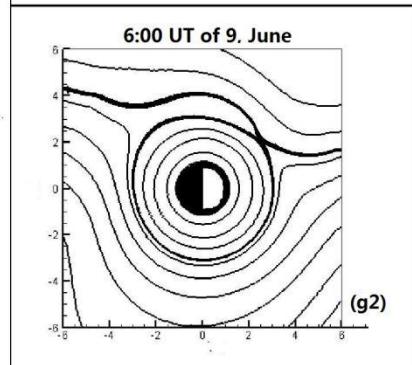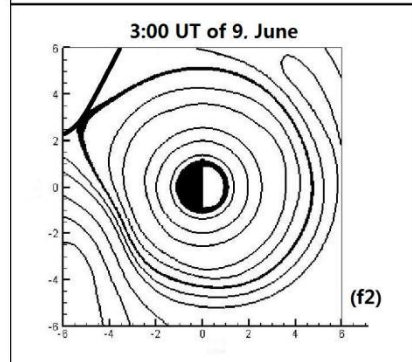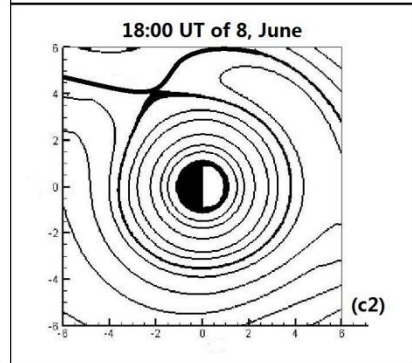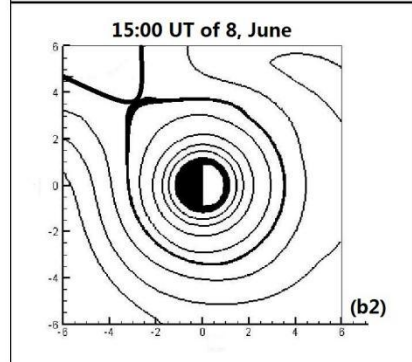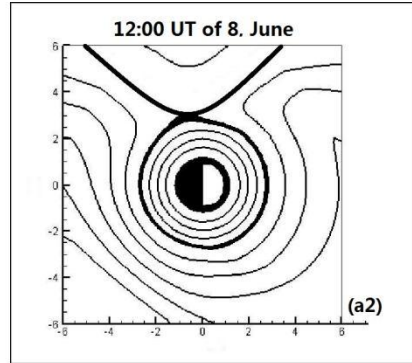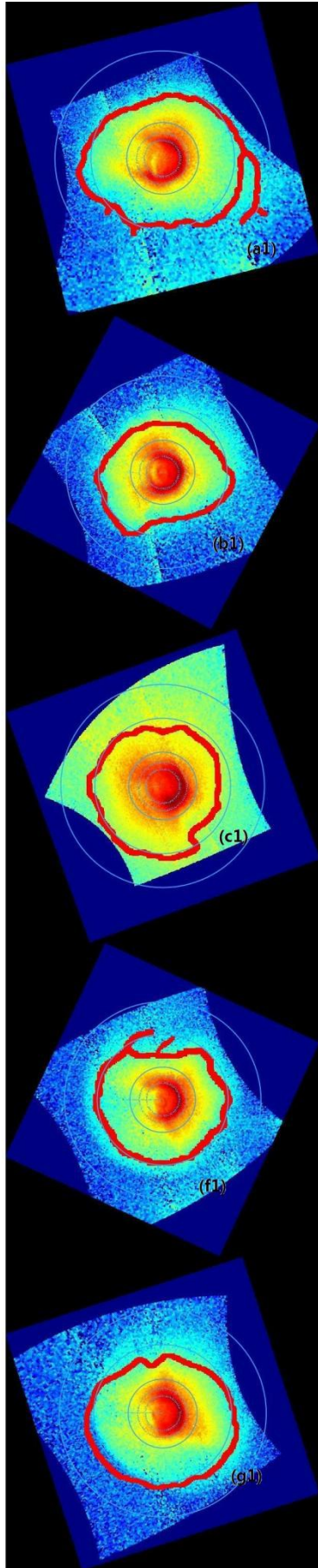
Figure 4. The subscript of panels correspond to Figure 3. The left column of panels show original observation results by EUV/IMAGE, the blue circles on the panels correspond to L=1, 2, 4 and 6. The right column of panels show equipotential lines in the equatorial plane, the last closed equipotential (LCE) is the bold black curve.

Panels of Fig.3(a) - (h) illustrate the plasmasphere obtained on the interval of from at 12:00 UT on 8 June to at 09:00 UT on 9 June in 2001 with snapshots every three hours. Figure4 illustrates original observations by EUV/IMAGE and equipotential lines in the equatorial plane. When the Kp index increased, the last closed equipotential shits closer to the Earth. The results of the simulation show the evolution and development of the features of the plasmapause, like shoulders and plumes. One can see that the plasmapause is closer to the Earth in the predawn sector. The reason is the increase of rotation velocity resulting in plasmapause of inward flow in the predawn sector (Pierrard and Cabrera, 2006; Verbanac et al., 2018). At 15:05 UT of 8 June, the TMP simulation captures an infant shoulder-like structure in panel Fig.3 (b), and then corotates with the plasmasphere body moved eastward and further reproduces a mature shoulder formation in Fig.3(c). The overall agreement between TPM simulation and EUV observed is quite well, but the TPM shoulder is located ~1.5 hours earlier in magnetic local time (MLT) that probably originated from the convection electric field model (Goldstein et al., 2002; Pierrard and Cabrera, 2005; Zhang et al., 2013).

The EUV observation illustrated in Fig.3 (f) shows that a plume is indeed observed in the afternoon or dusk sector. The results of the simulation also reproduce the formation and the evolution of the plumes, which derives from the shoulder structure in this case, illustrated in panels of Fig.3 (d)-(f). The simulation shows that the shoulders generate in the post-midnight sector (Verbanac et al., 2018), and then rotates eastward around the Earth to the afternoon sector (Goldstein et al., 2002). When the level of geomagnetic activity increases, the plasma element in the shoulder around the outer plasmasphere would convect outward and then into the dayside magnetopause (Li and Xu, 2005; Pierrard et al., 2008), and produce the plasmaspheric plume structure. The shoulder1 firstly arises on Fig.3(a) in the morning sector (at 12

167   UT, 8 June 2001), and then corotates with the main body of the plasmasphere to the

168   afternoon sector on Fig.3(c)(at 18 UT, 8 June 2001). During this period, the Kp index

169   increases to 3+ from 1 (see in Fig.2), and magnetosphere convection is slightly

170   enhanced that triggers plasma elements in the shoulder1 doing sunward convection,

171   then produces the plume1 at 21 UT on 8 June 2001 (see in Fig.3(d)). The mature

172   shoulder2, illustrated in Fig.3(b), corotates eastward with the Earth to the

173   afternoon-dusk sector. During the period of 0-3 UT on June 9, the Kp index gradually

174   increases up to 5+, indicating that magnetospheric convection is enhanced and the

175   convective electric field increases. The infantile plume2, illustrated in the panel of

176   Fig.3(e), derives from outflow of plasma elements in the shoulder2, and evolves into

177   the mature plume2 in Fig.3(f). Later, the double-plumes formation that is extended

178   from the plasmapause to the magnetosphere, is presented in the simulation results in

179   panels of Figs.3 (e)-(f).

180   The cavity in between the double plumes, or between plumes and the main body

181   of plasmasphere, may be responsible for the formation of channel and notch structures

182   (Gallagher et al., 2005). The base and the westward edge of the plume are connected

183   with the main body of plasmasphere. Moreover, there is a cavity topology, a

184   low-density region, between the tail structure of the plasmasphere and the main body

185   of plasmasphere. That is the channel structure of the plasmasphere. The plume

186   corotates with the Earth, becomes thinner, and finally disappeared (Li and Xu, 2005).

187   The results of simulation reproduce the channel structure in Fig.3(f). Gallagher et al.

188   (2005) proposes that notches and channels share the same origin, which derive from a

189   low-density cavity in the dusk region during recovery at the base of the plasmaspheric

190   plume. The absence of notch structure in this simulation event is due to the fact that

191   the potential structure does not cause the inward flow of plasma in the afternoon

192   sector, and the low disturbance time is maintaining for not long enough.

193   By contrastive analysis on between Fig.2 and Fig.3, the formation of the

194   shoulder is produced during the intensity of the convection electric field suddenly

195   decrease (Goldstein et al., 2002; Pierrard and Lemaire, 2004), when IMF sudden turns

196   northward from southward. There are three shoulders reproduced during this substorm

197 period, depicted in panels of Fig.3 (b)-(g). The time of the shoulder appearance is

198 labeled by three red circles in Fig.2, at 14:00 UT, 17:00 UT, 23:00 UT on 8 June

199 respectively. At that moment, the Bz component of the IMF turns northward. But not

200 all of the times, the Bz component of the IMF that turns northward could produce the

201 shoulder structure. One can see that no shoulders were reproduced in the results of the

202 simulation, at 02:00 UT, 05:00 UT, and 08:00 UT on 9 June 2001 respectively. The

203 Bz value of southward component must be less than the previous 24-hours mean

204 value. The intensity of the convection electric field is greater than the previous

205 24-hours level. So the last closed equipotential line (LCE) would be closer to the

206 Earth and result in plasmapause of inward flow in the predawn sector (Zhang et al.,

207 2013).

4. **Discussion**

209 The physical explanation of shoulder formation is not yet understood. In the present

210 section, we use the case of Figure 1 as an example to investigate the physical

211 mechanism of shoulder formation based on the TPM model. Fourteen test particles

212 are placed in the range of $2.5 \leq L \leq 3.8$, initial position located at 12:00 MLT, space step

213 takes 0.1Re, and then trace these particles' motion. Outputs are the trajectory (see in

214 Fig.5(a)) and the rotation rate (see in Fig.5(b)) of these test particles corresponding to

215 given magnetic local time illustrated in the bottom of Fig.5.
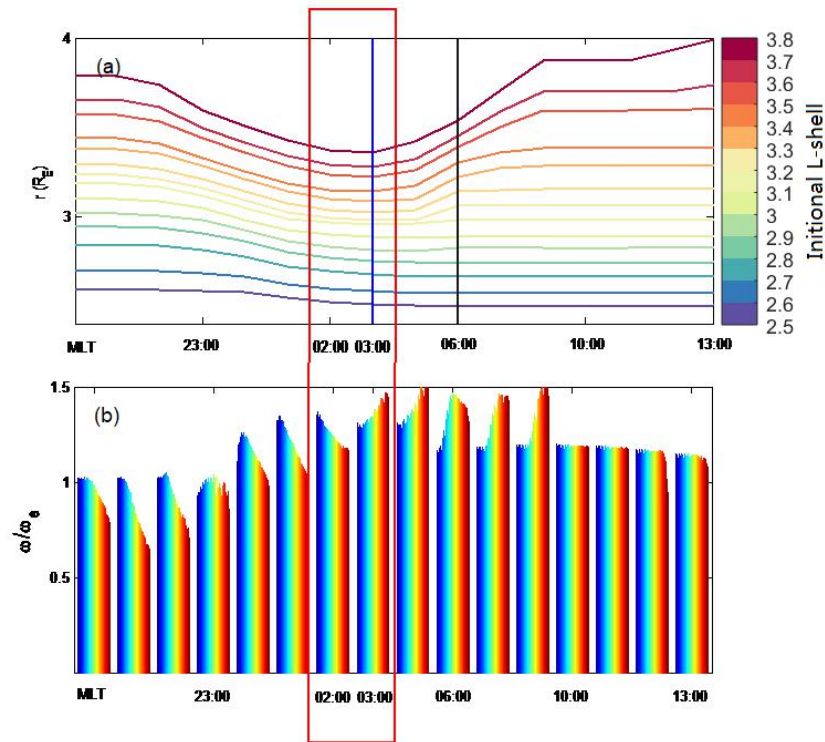
Figure 5. The trajectory (upper plot) and the rotation rate (bottom plot) of 14 test particles corresponding to MLT (location-dependent) during a substorm. The legend indicates fourteen test particles of various initial L-shell. The day is 8 June 2001.

The top panel shows that the outer part of plasmasphere (L>3.3 Re) drifts inward before 02 MLT, and moves outward (could reach up to 3.9 Re position) in the predawn sector (after 03:00MLT sector) (Verbanac et al., 2018). The radial motion of inner plasmasphere (L<3.3) is negligible. The shoulder is forming across 03-06 MLT region (between blue vertical line and black vertical line in Figure 5(a)). The outermost particle moves outward 0.7 Re, and the fourth particle moves outward 0.45 Re, from 03:00 MLT to 08:00 MLT. So, the shoulder has a sharp eastern edge about 0.2Re~0.3Re in radial extension and across a narrow 3-5 hours MLT region. Goldstein et al.(2002) proposed the shoulder formation by an outward radial motion of plasma in a narrow range and in the morning sector. The simulation of this paper verifies the conclusions of Goldstein (2002) and Verbanac (2018).

The lower panel shows the corotational angular velocity of test particles in the range of 2.5 < L< 4.0. The simulation results suggest that plasma element in

233 plasmasphere region rotation speed varies significantly with radial distance (Galvan,

234 2010). The inner part of plasmasphere rotates faster than its outer part before 02:00

235 MLT sector, vice versa in a range of in the 03:00-08:00 MLT sector [Lejosne and

236 Mozer, 2016]. The previous researchers analyzed the EUV observation and proposed

237 the shoulder structure has MLT sharpening in the angular direction. It indicates that

238 the outer edge of the shoulder rotates faster than the inner edge, resulting in

239 steepening of the MLT-profile of the shoulder (Goldstein et al., 2002). The lower

240 panel shows, with the increase of L, the rotation rate of the plasmasphere tends to

241 slightly decrease on the dusk side and obviously increase on the dawn side.

242   Fig. 5 indicates, in the region of 21:00 - 23:00:00 MLT, that the rotation rate is

243 about corotation in the inner plasmasphere (L<3), but is the interval of 70% - 90% of

244 corotation in the outer plasmasphere (L>3). The rotational value decreases with the

245 increase of L [Galvan et al., 2010]. Gallagher et al. (2005) investigates the drift rate of

246 notches in the geomagnetic quite phase, and the results show that the average rotation

247 rate of plasmasphere is about 90% of the corotational rate, in agreement with the

248 results of Lejosne and Mozer (2016). When the plasma elements rotate to the region

249 of 23:00 - 02:00 MLT, rotation rate in the outer plasmasphere reaches ~ 130% of

250 corotation, and in the inner plasmasphere is also close to the corotation rate. The

251 results show that the rotation rate of plasmasphere is overall increasing in the region.

252 In addition, the plasma elements in the outer plasmasphere rotate faster than the inner

253 plasmasphere in this region. The Fig.5(b) shows that rotation rate in the outer

254 plasmasphere highly reaches ~ 140% of corotation, and rotation rate in the inner

255 plasmasphere is close to 110% of corotation. So, we propose that the physical

256 mechanism of the shoulder formation is plasma extrusion of outer plasmasphere in the

257 predawn sector, due to outer plasmasphere both drifts radial outward and rotates faster.

258 In the present paper, the results show that the rotation rates of simulation are higher

259 than the observations, and not consistent with Huang et al. (2011) and Galvan et al.

260 (2010). The first reason is that this is a substorm case, so the convection of

261 magnetosphere is greater than the previous study articles of the geomagnetic quiet

262 case. (Galvan et al., 2010; Huang et al., 2011; Verbanac et al., 2018). The second

reason is that the Weimer electric field model is larger in practice, which results in a larger total electric field value in calculation (Goldstein et al., 2002; Pierrard et al., 2008).

The dawn-dusk asymmetry of convective electric field is caused by the terminal conductivity gradient of the ionosphere. The subrotation of the ionosphere drives the subrotation of the plasmasphere, and the plasmaspheric drift is correlated with the phase of geomagnetic storm (Burch et al., 2004). The convection electric field of Weimer (2001) is obvious dawn-dusk asymmetry, that causes a smaller increase on the dawnside and a lager decrease on the duskside, indicating that the subrotational effect of the plasmasphere is modulated by field-aligned current changes and conductance variations (Liemohn et al., 2004). The asymmetry of potential pattern causes the sunward convection in the magnetospheric night-side to be larger than that in the morning side, resulting in the subcorotational flow in the dark side. (Gallagher et al., 2005).

5. Conclusion

In this paper, we simulated the case of substorm on 8 June 2001 to investigate the physical mechanism of the shoulder formation based on TPM model that utilizes Weimer's electric field and the drift motion theory. We use the E-model and the B-model that are qusi-static background field and global averages. So, the results of simulation have some deviations with EUV observation. But, we have satisfactorily reproduced the evolution and development of the features of the plasmapause, like the shoulders and plumes. And then, the physical mechanism of the shoulder formation has been investigated.

The formation of shoulder is associated with IMF northward turning in the predawn sector. And the physical mechanism of shoulder formation is the result of plasma extrusion in the predawn sector, caused by the fact that outer plasmasphere drifts radially outward and rotates faster. The corotation rate in midnight sector decreases with the increasing L-shell, while it increases in pre-dawn sector. So, the shoulder

292 forms across in the 03-06 MLT region.

293   The formation and evolution of plume and channel have also been reproduced in

294 this case. One can see single or double plumes appear in the dusk or afternoon sector,

295 then become thinner with time, and finally disappear.

296   In this model, we do not consider the refilling process of the ionosphere. In the

297 future work, the refilling process should be considered, and we expect to obtain more

298 reasonable results. And also, the physical mechanisms of plasmaspheric features

299 observed by EUV/IMAGE, like notch or channel, also are to be investigated by TPM

300 model in future work underway.

301 **Author contributions:** Zhang H. conceptualized the project and wrote the original

302 draft of the paper. Peng G. S. modified the Figures and coded the Fortran program. Shen

303 C. supervised the project, and reviewed and edited the paper. Wu Yewen gives some

304 suggestions and draws Figure 4 for the paper.

305

306 **Acknowledgment**: The author thanks the professor D. R. Weimer, who provided the

307 code of Weimer's electric field model and ACE satellite data center and Word Data

308 center for Geomagnetism, Kyoto provided observation data. The dataset of

309 EUV/IMAGE could be downloaded from the website http://euv.lpl.arizona.edu/euv.

310

311 **References**

312 Burch, J. L., Mende, S. B., Mitchell, D. G., Moore, T. E. , Pollock, C. J., Reinisch, B.

313 W., Sandel, B. R., Fuselier, S. A. , and Gallagher D. L.: Views of Earth's

314 magnetosphere with the IMAGE satellite, Science, 291, 691-624, doi:

315 10.1126/science.291.5504.619, 2001.

316 Carpenter, D. L. and Anderson, R. R.: An ISEE/Whistler model of equatorial

317 electron density in the magnetosphere, J. Geophys. Res., 97, 1097-1108,

318 doi:10.1029/91JA015481992, 1992.

319 Chen, A. J. and Wolf, R.A. : Effects on the plasmasphere of a time-varying convection

320 electric field, Planet. Space Sci., 20, 483-509, doi: 10.1016/0032-0633(72)90080-3,

321 1972.

322 Gallagher, D. L., Adrian, M. L. and Liemohn, M. W.: Origin and evolution of deep

323 plasmaspheric notches, J. Geophys. Res., 110, A09201, doi:10.1029/2004JA010906,

324 2005.

325 Galvan, D. A., Moldwin, M. B., Sandel, B. R., and Crowley, G. : On the cause of

326 plasmaspheric rotation variability: IMAGE EUV observation, J. Geophys. Res., 115,

327 A01214, doi:10.1029/ 2009JA014321, 2010.

328 Goldstein, J., Spiro,R. W., Reiff, P. H., Wolf, R. A., Sandel, B. R., Freeman, J. W., and

329 Lambour, R. L.: IMF-driven overshielding electric field and the origin of the

330 plasmaspheric shoulder of May 24, 2000, Geophys. Res. Lett., 29(16), 1819,

331 doi:10.1029/2001GL014534, 2002.

332 Grebowsky, J. M.: Model study of plasmapause motion, J. Geophys. Res., 75,

333 4329-4333, doi:10.1029/JA075i022p04329, 1970.

334 Huang Y., Xu, R. L., Shen, C., and Zhao H.:   Rotation of the Earth's plasmasphere at

335 different radial distances, Adv. Space. Res., 48, 1167-1171, doi:

336 10.1016/j.asr.2011.05.028, 2011.

337 Lejosne, S., and Mozer, F. S. : Van Allen Probe measurements of the electric drift

338 $E×B$/B^2 at Arecibo's L=1.4 field line coordinate, Geophys. Res. Lett., 43, 6768-6774,

339 doi: 10.1002/2016GL069875, 2016.

340 Li, L., and Xu, R. L.: Model of the evolution of the plasmasphere during a

341 geomagnetic storm, Adv. Space. Res., 36, 1895-1899. doi: 10.1016/j.asr.2003.10.057,

342 2005.

343 Nishida A.: Formation of plasmapause, or magnetospheric plasma knee, by the

344 combined action of magnetospheric convection and plasma escape from the tail, J.

345 Geophys. Res., 71, 5669-5679, doi:10.1029/JZ071i023p05669, 1966.

346 Pierrard V., and Lemaire, J. F.: Development of shoulders and plumes in the frame of

347 the interchange instability mechanism for plamapause formation, Geophys. Res. Lett.,

348 31, L05809, doi:10.1029/2003GL018919, 2004.

349 Pierrard, V., and Cabrera, J.: Comparisons between EUV/IMAGE observations and

350 numerical simulations of the plasmapause formation, Annales Geophysicae, 23,

351 2635-2646, doi:10.5194/angeo-23-2635-2005, 2005.

352 Pierrard, V., and Cabrera, J.: Dynamical simulations of plasmapause deformations,

353 Space.Sci.Res, 122, 119-126, doi: 10.1007/s11214-006-5670-3, 2006.

354 Pierrard, V., Khazanov, G. V., Cebrera, J., and Lemaire, J.: Influence of the convection

355 electric field models on predicted plasmapause positions during magnetic storms. J.

356 Geophys. Res. 113, A08212, doi:10.1029/2007JA012612, 2008.

357 Sandel, B. R., King, R. A., Forrester, W. T., Gallagher, D. L., Broadfoot, A. L., and

358 Curtis, C. C.:   Initial results from the IMAGE extreme ultraviolet imager, Geophys.

359 Res. Lett., 28, 1439, doi: 10.1029/2001GL012885, 2001.

360 Verbanac, G., Bandic, M., Pierrard, V., and Cho, J.: MLT plasmapause characteristics:

361 Comparison between THEMIS observations and numerical simulations. J. Geophys.

362 Res: Space physics, 123, 2000-2007, doi:10.1002/2017JA024573, 2018.

363 Weimer, D. R.: An improved model of ionospheric electric potentials including

364 substorm perturbations and application to the Geospace Environment Modeling

365 November 24, 1996, event., J. Geophys. Res., 106, 407-416,

366 doi:10.1029/2000JA000604, 2001.

367 Zhang, H., Xu, R. L., Zhao, H., and Shen, C.: The characteristics of the model of

368 Weimer's electric field within the magnetosphere., Chinese J. Geophys. 55, 36-45, doi:

369 10.6038/j.isnn.0001-5733.2012.01.004, 2012.

370 Zhang, H., Xu, R. L., Shen, C., and Zhao, H.: The simulation of the plasmaspheric

371 morphology during a magnetospheric disturbance event, Chin J. Geophys, 56,

372 731-737, doi:10.6038/cjg 20130302, 2013.